iMEDiTEC 2017

ORIGINAL PAPER

The Effect of Flow Rate Characteristic on Biodegradation of Bone Scaffold

Hasan Basri [a,*], Jimmy D. Nasution[a], Ardiyansyah Syahrom[b,c], M.A. Sulong[b,c], Amir Putra Md Saad[b], Akbar Teguh Prakoso[a], Faisal Aminin[a]

[a] *Departement of Mechanical Engineering, Faculty of Engineering, Universitas Sriwijaya, Kabupaten Ogan Ilir, Palembang, Sumatera Selatan, Indonesia*
[b] *Department of Applied Mechanics and Design, Faculty of Mechanical Engineering, Universiti Teknologi Malaysia, 81310 Johor, Malaysia*
[c] *Sports Innovation and Technology Centre (SITC), Institute of Human Centred and Engineering (IHCE), Universiti Teknologi Malaysia*

* *Corresponding author: hasan_basri@unsri.ac.id*

ABSTRACT

This paper proposes an improved modeling approach for bone scaffolds biodegradation. In this study, the numerical analysis procedure and computer-based simulation were performed for the bone scaffolds with varying porosities in determining the wall shear stresses and the permeabilities along with their influences on the scaffolds biodegradation process while the bio-fluids flow through within followed with the change in the flow rates. Based on the experimental study by immersion testing from 0 to 72 hours of the time period, the specimens with different morphologies of the commercial bone scaffolds were collected into three groups samples of 30%, 41%, and 55% porosities. As the representative of the cancellous bone morphology, the morphological degradation was observed by using 3-D CAD scaffold models based on microcomputed tomography images. By applying the boundary conditions to the computational fluid dynamics (CFD) and the fluid structure interaction (FSI) models, the wall shear stresses within the scaffolds due to fluid flow rates variation had been simulated and determined before and after degradation. The increase of fluid flow rates tends to raise the pressure drop for scaffold models with porosities lower than 50% before degradation. As the porosities increases, the pressure drop decreases with an increase in permeability within the scaffold. The flow rates have significant effects on scaffolds with higher pressure drops by introducing the wall shear stresses with the highest values and lower permeability. These findings indicate the importance of using accurate computational models to estimate shear stress and determine experimental conditions in perfusion bioreactors for tissue engineering more accurate results will be achieved to indicate the natural distributions of fluid flow velocity, wall shear stress, and pressure.

INTRODUCTION

In the field of clinical health, many studies have been carried out for finding the materials that have the natural potential of reformation process of damaged or missing bone tissue. Some of those have demonstrated the study results indicated that the preponderance of Hydroxyapatite and Tricalcium Phosphate among bio-ceramics material was delivering a higher increase of biocompatibility, osteoconductivity, osteoinductivity, and similarity of material surface chemistry to the natural bone [1], [2]. As well as for load bearing application, biocompatible metallic scaffolds made of stainless steel, titanium alloys, and NiTi have given the expectation to fulfill the required mechanical strength [3].

Apart from biomaterial compatibility with biological environment, many requisites should be met through the micro- and macro-scale design of a porous structure in scaffolds [4], [5]. When it comes to the morphological design, the biomechanical modulation involving with simultaneous consideration of structural and bio-fluidic properties is becoming a vital aspect [6]. From a microscopical point of view, although the main topological features having the significant impact on biological efficiency has been frequently addressed, there are still conflicts between reported data [7]. The minimum pore size of 80 µm has been found to be necessary for an optimum cell penetration in Hydroxyapatite scaffolds [8]. Some studies also have found the suggested pore sizes with the values higher than 300 µm could enhance cell proliferation [9], [10]. Nevertheless, Murphy *et al.* [11] had stated that although there was a higher bone formation within scaffolds with 325 µm of pore size, the pore size of 120 µm also showed considerable early additional peak. In addition, a substantial capillary density was reported for pore sizes higher than 140 µm [12] and in the range 300-1200 µm no considerable difference was found in bone formation [13]. As well, in terms of porosity, the values higher than 85% was seen to improve cell penetration up to 400 µm [14] whereas the porosities larger than 75% was suggested to ensure cell proliferation [15], [16]. Furthermore, Danilevicius *et al.* [17] observed a higher efficiency for the scaffold with the 86% porosity compared the ones with 82% and 90%. Given this disparity and complication, many attempts have been made to quantitatively describe permeability of porous scaffolds to conglomerate main topological features such as porosity, pore architecture, pore size, and interconnectivity through which biological efficiency of pore morphology is being characterized [18], [19], [20], [21]. The recent study performed by Syahrom *et al.* [22] had offered that prismatic plate suggested as a rod model has shown the similar permeability as of natural bone and the higher permeability was attributed to structures comprised of tetrakaidecahedron unit cells. The accuracy of CFD calculations in predicting permeability of regular scaffolds was also studied by Truscello *et al.* [23] and their results were in good agreement with the experimental data by less than 27% of error.

The principal tissue of metallic implants is their loosening due to bone resorption caused by stress shielding, weak interfacial bonding between the implant and the bone, and the lack of biological anchorage for growing tissues [24]. To address these issue, there has been so much effort on the development and characterization of metal

eISBN 978-967-0194-93-6 FBME

implants with microstructures and properties closer to those of cancellous bones. Accordingly, these materials are called open-cell porous metals, metallic foams, metallic scaffolds, or cellular metals with three-dimensional interconnected pores. The pore sizes are typically between 200 and 500 μm with a total porosity of 50-75% [25]. For this purpose, the metal is made porous to provide a scaffold for the bone tissue to grow into and through the pores thus making a suitable bond to the metallic implant [26]. Present tissue engineering approaches are focused on the development of porous scaffolds made of different porosity with the aim of analyzing fluid characteristic when the scaffold has been implanted in tissue body

Fluid flow is primarily caused by compressive loading of bone as a result of physical activity. Changes in loading, e.g., due to extended periods of bed rest or microgravity in space are associated with altered bone remodeling and formation in vivo. In vitro, it has been reported that bone cells respond to fluid shear stress by releasing osteogenic signaling factors, such as nitric oxide, and prostaglandins [27].

Evaluating fluid flow mechanism and subsequently, permeability [28] or wall shear stress [29] is an important part because of the direct effects of these parameters on cell bioactivity within scaffolds, especially in perfusion bioreactor system. A permeable scaffold should allow efficient nutrient and gas diffusion and waste emission through its channels [30]. Determining scaffold permeability is an important factor in predicting cell proliferation, regardless of the fact that permeability can exert opposite effects on different types of cells [31]. Appropriate cellular signals, including those induced by biophysical stimulants, enable the formation of desired tissue inside a scaffold's pores [32]. Among the well-known biological stimulants, the shear stress that arises from fluid flow exert the most pronounced effect [33].

A number of studies have been conducted to investigate factors that effectively control permeability and wall shear stress. O'Brien *et al*. carried out experimental and mathematical analysis and found that scaffold permeability depended mainly on porosity [34]. Another study probed into the effect of porosity and pore size on permeability through an experiment and computational analysis [18]. The result showed that the permeability improved with increasing porosity and pore size. Given major role of fluid flow rates in WSS, numerous studies have focused on flow-induced shear stresses [33], [35]. Bartnikowski *et al*. probed into the effects of scaffold architecture with a porosity of 60% on osteoblast response in perfusion bioreactor and static cell cultures [29]. It was found good agreement in the permeability results derived from CFD and experiments, it was concluded that CFD analysis is a reliable tool for predicting WSS. Zhao *et al*. performed CFD analysis to investigate the effect of geometrical parameters, such as pore size and shape on WSS [36]. Their finding indicated that pore size more significantly influenced mechanical stimulation within a scaffold than the structural architecture and porosity. In a recent study, the different ranges of WSS were obtained only by modifying scaffold architecture [32].

Physiological activity is very important for bone homeostasis. The generated mechanical loading from physiological activity induces a mechanical stimulus of fluid flow [37] due to pressure differentials. Routine physical activities such as walking, jogging, stair-climbing, and stumbling result in different loadings on the human bone. The average loading during walking, jogging and fast walking, stair climbing, and stumbling are 3.1 x body weight (BW), 6.2 BW, and 8.7 BW, respectively. The BW is based on a 75 kg [27], [28]. These variations in mechanical loading generate different bone strains (1000-3500 με) that create the pressure difference in bone [29]. Consequently, different flow rates induce different flow rates of the bone marrow are generated. These variations in flow rates induce different shear stress levels that are experienced by bone cells [30]. Mechanical stimulation demonstrates better osteogenic differentiation than static culture because bone cells are subjected to fluid flow [31], [32]. Thus, it is necessary to consider the mechanical stimulus of fluid flow in determining the degradation behavior of porous Mg in immersion tests.

To address this gap, the current study carried out computational simulation base on CFD and FSI to determine the effects of different porosity scaffold architecture on physical of human activity and its biodegradation.

MATERIALS AND METHOD

Previous research overview

Cuboid-shaped (5 x 5 x 3 mm) of commercially available pure magnesium (rod diameter of 24.4 mm and 99.9% purity which was made by Good Fellow Inc, Cambridge, UK) having interconnected holes were fabricated using CNC machine (HAAS, USA). The samples were drilled using a drill bit of 800 μm diameter. The porous magnesium of bone scaffold with varying porosity and surface area can be shown in Fig. 1c [38]. The morphological of the specimens are shown in Table 1.

The three groups of specimens with different morphologies were labeled as sample A, B, and C. The samples were fabricated with three different porosities 30%, 41%, and 55% respectively which were selected on the basis of the morphology of cancellous bone. For the experimental test, there were 27 porous magnesium samples were prepared within the scope of this research. The different flow rates of bone marrow across a cancellous bone structure were translated to an *in vitro* experimental setup, as shown in Figure 1a and 1b [38]. A laminar flow in a channel with a 41-mm length (L) was set. Three different flow rates i.e 0.025, 0.4 and 0.8 ml/min respectively to perform different mechanical loadings. A chamber was specifically designed with a 2 mm diameter (D) to clamp and hold the specimen in the channel during testing. Two pressure gauges (EMA, China) were placed before and after the chamber to measure the pressure difference in which both were connected to a data acquisition instrument (DAQ, National Instruments, USA). The porous Mg was subjected to immersion tests for the periods of 24, 48 and 72 hours. Once tested, the specimen removed from the chamber, gently rinsed with deionized water, and then dried under vacuum for 1 hour.

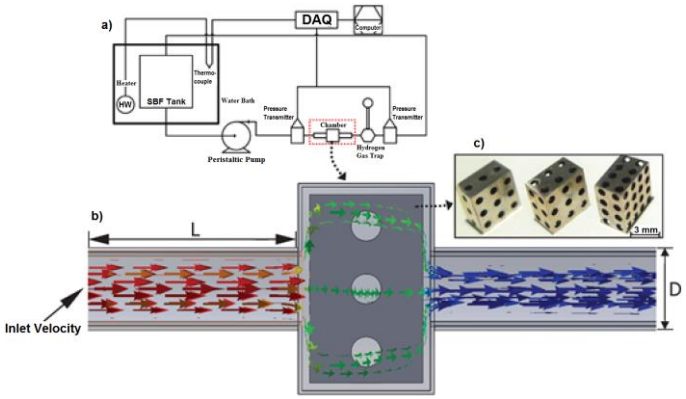

Fig. 1 a) and **b)** The dynamic immersion test rig system, **c)** Three different morphology of bone scaffolds [38].

Table 1 Morphologic details of porous magnesium scaffold specimens [38].

Type	Porosity	Surface Area	Volume	Surface area per volume
A	30%	189.30 mm^2	52.87 mm^3	3580.48 m^{-1}
B	41%	209.81 mm^2	44.57 mm^3	4704.43 m^{-1}
C	55%	225.75 mm^2	33.83 mm^3	6673.07 m^{-1}

Three Dimensional Model Preparation

In order to determine the behavior of fluid flow of porous magnesium scaffold, computer aided design (CAD) models of bone scaffold initially were generated using Solidworks modeling software as shown in Figure 2. One sample from each porosity (i.e. A, B, and C) and each immersion group (i.e. 24, 48 and 72h) with 0.025 ml/min

eISBN 978-967-0194-93-6 FBME

flow rate, were scanned by means of the micro-computed tomography (µCT) device. For simulation purpose, there only 9 samples were scanned. Raw images with a resolution of 17.20 µm by using a µCT scanner (Skycan 1172, Kontich, Belgium) were taken. In general, µCT data sets provide spatial information, suitable for measurements of various bone parameters such as bone volume, bone thickness bone mineral density and surface area.

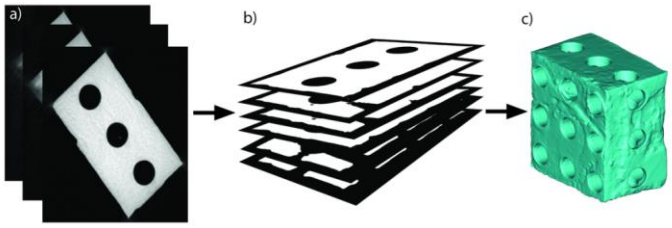

Fig. 2 Illustration of the preparation process of bone scaffold reconstruction: a) raw data µCT, b) segmentation of images stacks and c) 3D model reconstruction.

The process to obtain a three-dimensional model from raw µCT images of the bone scaffold is illustrated the step-by-step process in Fig. 2. Representative cross-sectional images of the specimen after degradation is shown in Fig. 2a. The data from µCT scan was processed by using the so-called gray value thresholding. The most important part of this step is to differentiate between the solid phase (i.e. specimen) from the air. After that, the raw data images are transformed into a binary form or simply black and white voxel and the scale of images have a setup with the true scale. The white voxel in the micrograph is grouped into the solid phase while a black voxel represents the air. Segmentation or thresholding procedure is conducted by using ImageJ software commands to set the right value of gray scale. ImageJ provides global thresholding algorithms by means of the plugin named Auto Threshold. In this study, automatic thresholding algorithm based on the Otsu's method was available in ImageJ is the best methods to show good agreement with the interactive method performed by the consultant. The raw threshold images data has been shown in Fig.2b and saved in (8-bit TIFF) format images. Finally, the raw data images after segmentation were exported into MIMICS software and the three-dimensional volume rendering was obtained with the 3D mask calculate using software command (see Fig. 3). Reconstructed 9 samples of porous magnesium specimens were exported as stereolithography format (STL) that indicate surface mesh. The STL surface mesh contains a large of number of triangles to avoid the loss of geometric details.

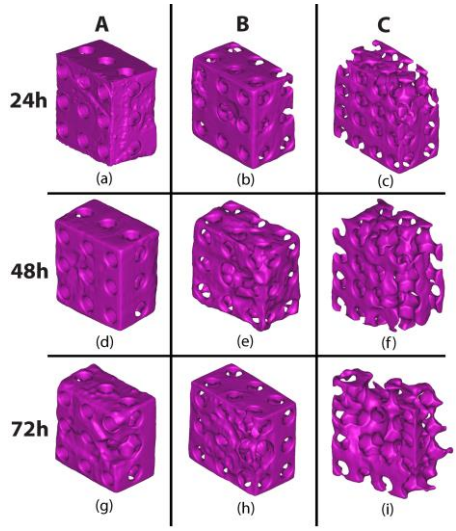

Fig. 3 Photograph comparison morphology between true samples and 3D reconstructed models of bone scaffold after biodegradation.

Boundary condition and material input

In the next step, the commercial software, COMSOL was used to transform the surface mesh into the volume mesh. The resulting numerical three dimensional contains tetrahedral elements. For fluid characterization of the porous magnesium scaffold specimen by using CFD, incompressible fluid properties (i.e. simulated body fluid) was used in the scope of this investigation and the values were assumed to have a density ρ = 1000 kg/m^3 and dynamic viscosity μ = 0.001 Pa.s.

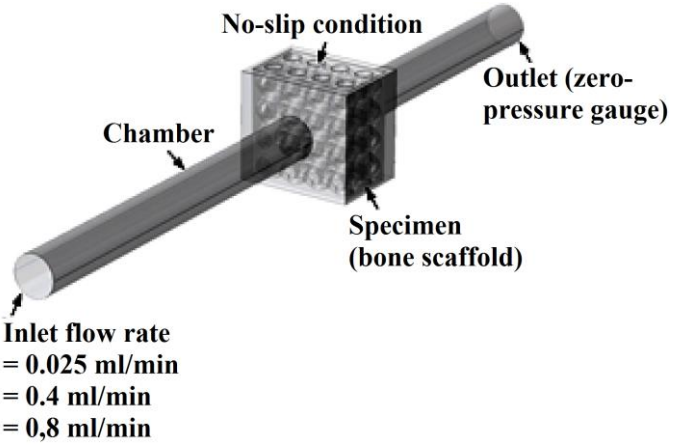

Fig. 4 The boundary conditions used in CFD simulation

CFD simulation procedure

The models for fluid flow analysis were solved by COMSOL solver. The properties of bio-fluid were set to 1000 kg/m^3 for density and 0.001 Pa.s for viscosity, respectively. In order to ensure the fluid flow remains laminar (satisfying Darcy's law), a low inlet flow rate was imposed at the inlet and zero pressure condition was defined at the outlet. Finally, the average pressure drop was obtained for each model and the permeability coefficient was calculated by Darcy's law using Eq. (1).

$$Q = \left(\frac{kA}{\mu}\right)\left(\frac{\Delta P}{L}\right) \quad (1)$$

Where Q is the volumetric flow rate, A is the cross-sectional area of the specimen (m^2), ΔP is set to the obtained pressure drop under defined boundary conditions (Pa), L is the specimen length (m), μ is the fluid viscosity, and k is the intrinsic permeability of the specimen. In order to exclude dimensional effects, the numerical permeability values were normalized by the permeability of a perfectly porous structure with the same boundary condition.

Mesh sensitivity study

A convergence study was performed where a minimum of 600,000 fluid cells was required for reliable results (see Fig. 5). The velocity value from the analysis had to be independent of mesh density, where the wall shear stress and permeability are directly dependent on the velocity. Roughly for the period of 2 hours were required to complete the generation of the mesh and another 3 hours were required to complete the simulation. All simulations were performed on a Dell Precision Workstation T54000 with Intel Xeon microprocessor and 128 GB of RAM.

RESULTS AND DISCUSSION

Many devices have been investigated for providing suitable mechanical stimuli to simulate the environment in vivo. The flow chamber used in the research was built to apply a steady fluid shear stress and permeability through scaffold in vitro. Since it was difficult

to validate the fluid wall shear stress generated with existing test methods, therefore a computational fluid dynamics was conducted. The SBF flowed through the flow chamber, generated fluid shear stress on the surface of the scaffold. The shear stress magnitude could be adjusted by changing the flow rate of the SBF solution.

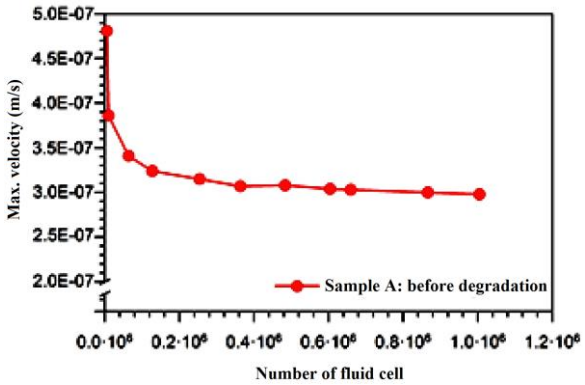

Fig. 5 Convergence study for fluid flow analysis

In order to determine the performance and reliability of the scaffold models in CFD analysis, their pressure drop (ΔP) responses to flow rate were tested under three different flow rates 0.025, 0.4 and 0.8 ml/min, respectively. From the CFD results for the three different scaffold porosities as shown in Fig. 6a, it was found that the pressure drop (ΔP) across the specimens increases linearly as the applied flow rate increases. The results sound good with the previously reported experimental work [23]. Thus, these results indicate that the simulation procedure followed the testing protocol.

The permeability of each specimen before degradation was then determined (see Fig. 6b). The influence of permeability of the specimen A (30% porosity), B (41% porosity), and C (55% porosity) under different flow rates does not significantly change. The specimen C has a higher permeability than the specimens A and B.

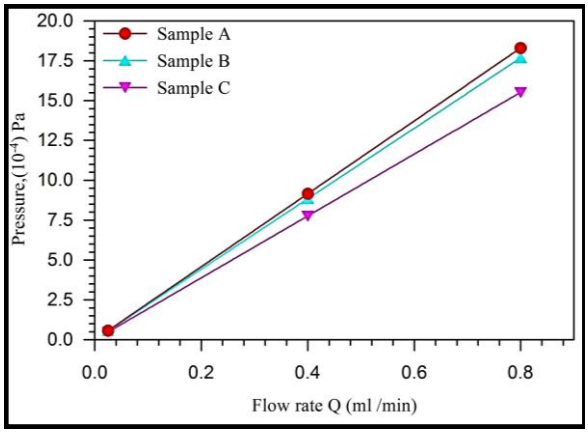

Fig. 6 (a) Relationship between pressure drop (ΔP) and flow rate (Q) before degradation.

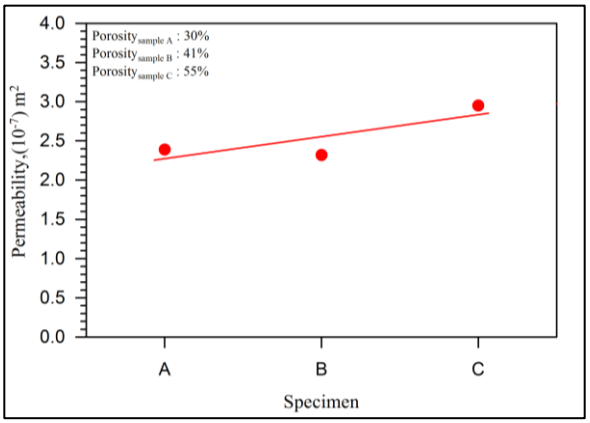

Fig. 6 (b) Permeability of bone scaffolds under three different flow rates before degradation.

A 2D middle cross-sectional was used to assess the shear stress of the specimen. The shear stress contour plot of the specimen under a flow rate of 0.025, 0.4 and 0.8 ml/min respectively was shown in Fig.7a. The contour plot shows the shear stress acted on the exposed surface was localized in the middle of the porous specimen. The wall shear stress at the middle of the porous structure of specimens A and B were shown to be higher compared to the specimen C. In order to determine the maximum localized wall shear stress at the porous structure for all specimens, the wall shear stress at the area marked with a* was selected. The average wall shear stress was then determined for each specimen under varying flow rates, as shown in Fig. 7b. The wall shear stress increased as the flow rate increased. The specimen B had a higher wall shear stress compared to the specimens A and C for all flow rates used. For example, the average wall shear stress for samples A, B, and C under the flow rate of 0.025ml/min are 0.152×10^{-5}Pa, 0.194×10^{-5}Pa, 0.16×10^{-5}Pa, respectively. From the simulation result, there is no correlation between shear stress and the porosity of bone scaffold.

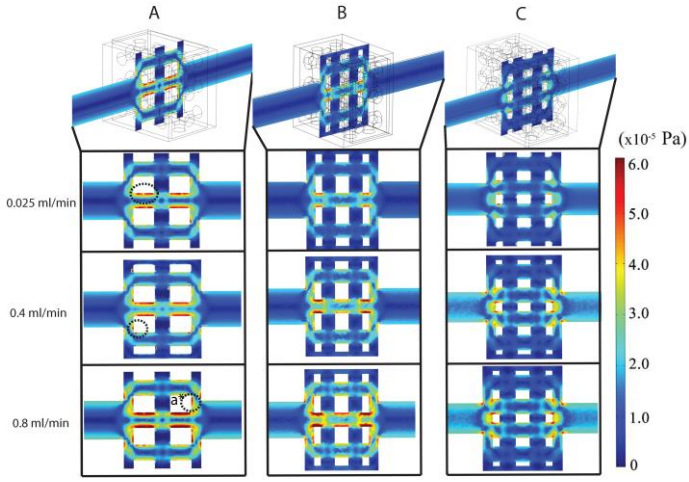

Fig. 7a The contour plot of shear stress on the porous scaffold specimens under different flow rates.

eISBN 978-967-0194-93-6 FBME

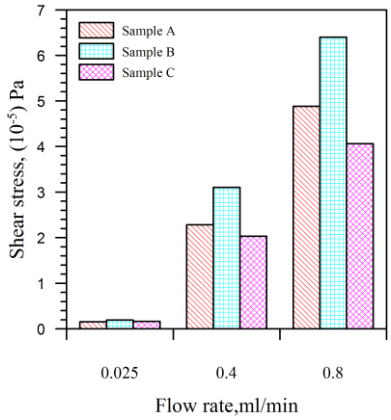

Fig. 7b The contour plot of shear stress on the porous scaffold specimens under different flow rates before degradation

The study on the permeability of idealized bone scaffold is as crucial as the mechanical properties, as it determines the capability of the idealized structure to pass nutrients through. A higher permeability value would allow a good supply of nutrients at the expense of the strength of the over all structure due to a high porosity value. Getting the right balance between permeability and mechanical strength is crucial to achieving the optimum performance of the idealized synthetic structure. As shown in Fig. 8, the permeability of the whole samples increased as the porosity increased. The 0h period indicated the sample before degradation and the 72h period indicated the sample after degradation. The significant level of the correlation was 0.58 for permeability and porosity. Although there are numerous reports on the permeability of porous structures, none have reported a study on scaffold samples before and after degradation using the computational method. The simulation results showed permeability graph similar to those found in previously reported experimental and simulation investigations [39], [40].

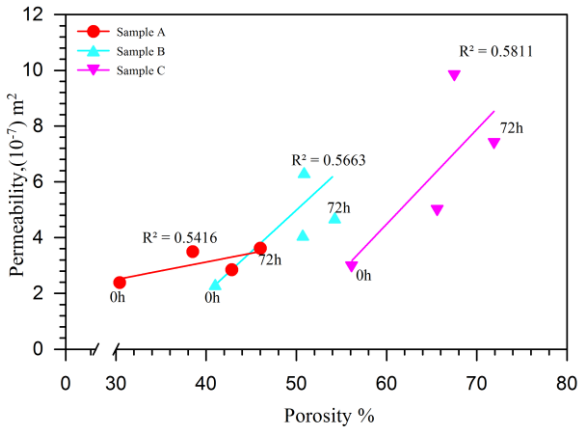

Fig. 8 The plot of permeability vs. porosity of bone scaffolds

Effect of the shear stress on biodegradation of bone scaffolds under the flow rate of 0.025 ml/min can be seen in Fig. 9. Firstly, after the specimen was subjected to simulated body fluid, the initial shear stress occurred and located in the middle of the scaffold which was seen from the color level. Within the period of 24 hours, the pores at the middle of the surface had been enlarged. As the degradation time increased, the pore size also increased. The relationship between the propagation of degradation and the maximum location of the fluid shear stress found in this study was in good agreement with previously reported experimental work on PLGA membrane [41]. Unfortunately, the high cost to carry out the specimen scan using µCT, the samples were subjected immersion test at a flow rate of 0.4 ml/min and 0.8 ml/min did not follow in this study.

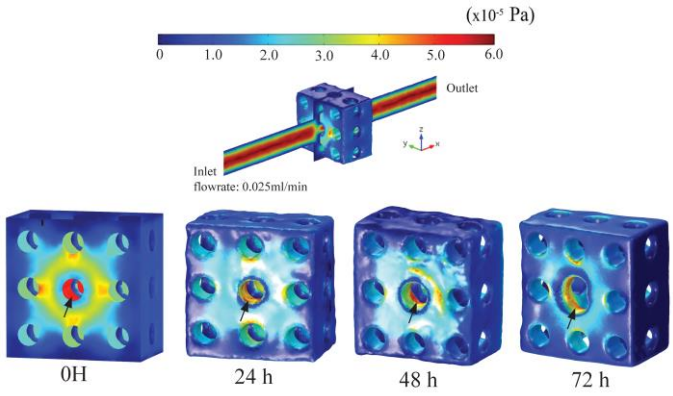

Fig. 9 Morphology of bone scaffold (sample A) before and after degradation under the flow rate of 0.025 ml/min.

CONCLUSION

The fluid shear stress has a great effect on the surface morphology of bone scaffold. This study is helpful for understanding the influence of the fluid shear stress on the in vitro degradation process of porous magnesium scaffold. The flow rates of bone scaffolds under physiological activities have been given the impact of the biodegradation and the effect of mass transport on the in vitro degradation process should be further investigated. It is deduced that the in vivo biodegradation of bone scaffold implants under fluid shear stress should be carefully considered to the advance appropriate degradation design for matching the healing or generation process in the biodegradable medical applications.

From the results and discussion above, it can be concluded as follows:

1. The wall shear stress increases as the flow rate increases.
2. The permeability increases as the porosity increases.
3. Effect wall shear stress on biodegradation has been fully developed, initial degradation refers to the location of wall shear stress.

Understanding the influence of fluid shear stress on the biodegradation of porous scaffold is helpful for effective prediction of the in vivo degradation dynamics, which is important in developing appropriate biodegradable medical implants and drug delivery system made of magnesium.

ACKNOWLEDGEMENT

This work was part of an International Research Collaboration between Universitas Sriwijaya, Indonesia and the Universiti Teknologi Malaysia, Malaysia.

REFERENCES

[1] J. Vivanco, A. Aiyangar, A. Araneda, and H. Ploeg, 2012. Mechanical characterization of injection-molded macro porous bio ceramic bone scaffolds. *J. Mech. Behav. Biomed. Mater.* 9, 137–152, 2012.

[2] C. Yu, N. Kikuchi, and S. J. Hollister, 2004. A novel method for biomaterial scaffold internal architecture design to match bone elastic properties with the desired porosity. *J. Biomechanics*. 37, 623–636, 2004.

[3] T. Bormann *et al.*, 2014. Acta Biomaterialia Combining micro computed tomography and three-dimensional registration to evaluate local strains in shape memory scaffolds. *Acta Biomater.* 10, 2, 1024–1034, 2014.

[4] H. A. Almeida and P. J. Bártolo, 2014. Medical engineering & physics design of tissue engineering scaffolds based on hyperbolic surfaces: a structural numerical evaluation. *Med. Eng. Phys.* 36, 8, 1033–1040, 2014.

[5] C. T. Koh, D. G. T. Strange, K. Tonsomboon, and M. L. Oyen, 2013.

Acta biomaterials failure mechanisms in fibrous scaffolds. *Acta Biomater.* 9, 7, 7326–7334, 2013.
[6] M. R. Dias, J. M. Guedes, C. L. Flanagan, S. J. Hollister, and P. R. Fernandes, 2014. Medical Engineering & Physics Optimization of scaffold design for bone tissue engineering: A computational and experimental study. *Med. Eng. Phys.* 36, 4, 448–457, 2014.
[7] Q. Zhang, H. Lu, N. Kawazoe, and G. Chen, 2014. Pore size effect of collagen scaffolds on cartilage regeneration. *Acta Biomater.* 10, 5, 2005–2013, 2014.
[8] F. R. Rose, L. A. Cyster, D. M. Grant, C. A. Scotchford, S. M. Howdle, and K. M. Shakesheff, 2004. In vitro assessment of cell penetration into porous hydroxyapatite scaffolds with a center aligned channel. *Biomaterials*. 25, 24, 5507–5514, 2004.
[9] V. Karageorgiou and D. K. Ã, 2005. The porosity of 3D biomaterial scaffolds and osteogenesis. *Biomaterials*. 26, 5474–5491, 2005.
[10] S. Lien, L. Ko, and T. Huang, 2009. Effect of pore size on ECM secretion and cell growth in gelatin scaffold for articular cartilage tissue engineering. *Acta Biomater.* 5, 2, 670–679, 2009.
[11] C. M. Murphy, M. G. Haugh, and F. J. O. Brien, 2010. Biomaterials The effect of mean pore size on cell attachment, proliferation, and migration in collagen – glycosaminoglycan scaffolds for bone tissue engineering. *Biomaterials*. 31, 3, 461–466, 2010.
[12] F. M. Klenke, Y. Liu, H. Yuan, E. B. Hunziker, K. A. Siebenrock, and W. Hofstetter, 2008. Impact of pore size on the vascularization and osseointegration of ceramic bone substitutes in vivo. *J. Biomed. Mater. Res. - Part A*, 85, 3, 777–786, 2008.
[13] S. J. Hollister, Engineering craniofacial scaffolds. *Orthodox. Craniofac. Res.*
[14] C. Ji, A. Khademhosseini, and F. Dehghani, 2011. Enhancing cell penetration and proliferation in chitosan hydrogels for tissue engineering applications. *Biomaterials*. 32, 36, 9719–9729, 2011.
[15] J. Zeltinger, D. Ph, J. K. Sherwood, D. a Graham, R. Müeller, and L. G. Griffith, 2001. Adhesion, Proliferation, and Matrix Deposition. 7, 5, 557–572, 2001.
[16] M. E. Gomes, H. L. Holtorf, R. L. Reis, and A. G. Mikos, 2006. Influence of the porosity of starch-based fiber mesh scaffolds on the proliferation and osteogenic differentiation of bone marrow stromal cells cultured in a flow perfusion bioreactor. *Tissue Eng.* 12, 4, 801–809, 2006.
[17] P. Danilevicius, L. Georgiadi, C. J. Pateman, F. Claeyssens, M. Chatzinikolaidou, and M. Farsari, 2015. The effect of porosity on cell ingrowth into accurately defined, laser-made, polylactide-based 3D scaffolds. *Appl. Surf. Sci.* 336, 2–10, 2015.
[18] M. R. Dias, P. R. Fernandes, J. M. Guedes, and S. J. Hollister, 2012. Permeability analysis of scaffolds for bone tissue engineering. *J. Biomech.* 45, 6, 938–944, 2012.
[19] C. Sandino, P. Kroliczek, D. D. McErlain, and S. K. Boyd, 2014. Predicting the permeability of trabecular bone by microcomputed tomography and finite element modeling. *J. Biomech.* 47, 12, 3129–3134, 2014.
[20] R. P. Widmer and S. J. Ferguson, 2012. On the interrelationship of permeability and structural parameters of vertebral trabecular bone: a parametric computational study. *Comput. Methods Biomech. Biomed. Engin.* 16, August 2014, 1–15, 2012.
[21] A. Rahbari, H. Montazerian, E. Davoodi, and S. Homayoonfar, 2016. Predicting permeability of regular tissue engineering scaffolds: scaling analysis of pore architecture, scaffold length, and fluid flow rate effects. *Comput. Methods Biomech. Biomed. Engin.* 5842, August, 1–11, 2016.
[22] A. Syahrom, M. Rafiq, A. Kadir, J. Abdullah, and A. Öchsner, 2013. Medical Engineering & Physics Permeability studies of artificial and natural cancellous bone structures. *Med. Eng. Phys.* 35, 6, 792–799, 2013.
[23] S. Truscello, G. Kerckhofs, S. Van Bael, G. Pyka, J. Schrooten, and H. Van Oosterwyck, 2012. Prediction of permeability of regular scaffolds for skeletal tissue engineering: A combined computational and experimental study. *Acta Biomater.* 8, 4, 1648–1658, 2012.
[24] G. Lewis, 2013. Properties of open-cell porous metals and alloys for orthopedic applications. 2013.
[25] B. B. Levine, 2008. A New Era in Porous Metals: Applications in Orthopaedics. 9, 788–792, 2008.
[26] A. H. Yusop, A. A. Bakir, N. A. Shaharom, M. R. A. Kadir, and H. Hermawan, 2012. Porous Biodegradable Metals for Hard Tissue Scaffolds: A Review. 2012, 2012.
[27] C. M. Perrault, 2016. In Vitro Bone Cell Models: impact of Fluid Shear Stress on Bone Formation. 4, November 2016.
[28] A. G. Mitsak, J. M. Kemppainen, M. T. Harris, and S. J. Hollister, 2011. Effect of polycaprolactone scaffold permeability on bone regeneration in vivo. *Tissue Eng. - Part A*, 17, 13–14, 1831–1839, 2011.
[29] M. Bartnikowski, T. J. Klein, F. P. W. Melchels, and M. A. Woodruff, 2014. Effects of scaffold architecture on mechanical characteristics and osteoblast response to static and perfusion bioreactor cultures. *Biotechnol. Bioeng.* 111, 7, 1440–1451, 2014.
[30] V. Serpooshan *et al.* 2010. The reduced hydraulic permeability of three-dimensional collagen scaffolds attenuates gel contraction and promotes the growth and differentiation of mesenchymal stem cells. *Acta Biomater.* 6, 10, 3978–3987, 2010.
[31] J. M. Kemppainen and S. J. Hollister, 2010. Differential effects of designed scaffold permeability on chondrogenesis by chondrocytes and bone marrow stromal cells. *Biomaterials.* 31, 2, 279–287, 2010.
[32] W. J. Hendrikson, A. J. Deegan, Y. Yang, C. A. Van Blitterswijk, and E. Farrell, 2017. Influence of Additive Manufactured Scaffold Architecture on the Distribution of Surface Strains and Fluid Flow Shear Stresses and Expected Osteochondral Cell Differentiation. *Front. Bioeng. Biotechnol.* 5, February, 1–11, 2017.
[33] R. Voronov, S. Van Gordon, V. I. Sikavitsas, and D. V. Papavassiliou, 2010. Computational modeling of flow-induced shear stresses within 3D salt-leached porous scaffolds imaged via micro-CT. *J. Biomech.* 43, 7, 1279–1286, 2010.
[34] F. J. O. Brien, B. A. Harley, M. A. Waller, and I. V Yannas, 2007. The effect of pore size on permeability and cell attachment in collagen scaffolds for tissue engineering. *Technol. Heal. Care.* 15, 3–17, 2007.
[35] A. Lehman, Y. Blinder, and S. Levenberg, 2010. Modeling of flow-induced shear stress applied on 3D cellular scaffolds: Implications for vascular tissue engineering. *Biotechnol. Bioeng.* 105, 3, 645–654, 2010.
[36] F. Zhao, T. J. Vaughan, and L. M. McNamara, 2016. Quantification of fluid shear stress in bone tissue engineering scaffolds with spherical and cubical pore architectures. *Biomech. Model. Mechanobiol.* 15, 3, 561–577, 2016.
[37] L. M. McNamara and P. J. Prendergast, 2007. Bone remodeling algorithms incorporating both strain and micro damage stimuli. *J. Biomech.* 40, 6, 1381–1391, 2007.
[38] N. Harun, H. Basri, J. Abdullah, and M. Rafiq, 2017. The Influence of flow rates on the dynamic degradation behavior of porous magnesium under a simulated environment of human cancellous bone. *Materials and Design.* 122, 268-279, 2017.
[39] C. G. Jeong and S. J. Hollister, 2010. Mechanical, permeability and degradation properties of 3D designed poly (1,8 Octanediol-co-Citrate) scaffolds for soft tissue engineering, *J. Biomed. Mater. Res. - Part B Appl. Biomater.* 93, 1, 141–149, 2010.
[40] H. Montazerian, M. Zhianmanesh, E. Davoodi, A. S. Milani, and M. Hoorfar, 2017. Longitudinal and radial permeability analysis of additively manufactured porous scaffolds: Effect of pore shape and porosity. *Mater. Des.* 122, 146–156, 2017.
[41] Z. Chu *et al.*, 2016. The effect of fluid shear stress on the *in vitro* degradation of poly (lactide-*co*-glycolide) acid membranes. *J. Biomed. Mater. Res. Part A.* 104, 9, 2315–2324, 2016.

eISBN 978-967-0194-93-6 FBME